The Egyptian Journal of Radiology and Nuclear Medicine (2016) 47, 711–721

Egyptian Society of Radiology and Nuclear Medicine

The Egyptian Journal of Radiology and Nuclear Medicine

www.elsevier.com/locate/ejrnm
www.sciencedirect.com

ORIGINAL ARTICLE

# Recent advances in MRI in the preoperative assessment of anorectal malformations

**Rania Farouk Elsayed, Heba Ahmed Kamal *, Nevien E. El-Liethy**

*Department of Radio Diagnosis, Faculty of Medicine, Cairo University, Egypt*

Received 6 April 2016; accepted 28 May 2016
Available online 15 June 2016

**KEYWORDS**

MRI;
Preoperative;
Anorectal malformations

**Abstract** *Objective:* To prospectively evaluate the diagnostic accuracy of triplanar 2D magnetic resonance (MR) images versus the post processing reconstructed MR images generated from a single 3D VISTA sequence in children with anorectal malformations compared with the operative findings as the Golden standard.

*Materials and methods:* This study had institutional review board approval, and informed consent was obtained from all participants. There were 20 patients with anorectal anomalies age range (2 months–3.5 years), referred from the pediatric surgery unit for preoperative MRI. The 2D sequences included Coronal TSE T2 WI parallel to the plane of the anal canal as seen on the sagittal images, and Axial TSE T2 WI oblique, perpendicular to the coronal plane. Sagittal T2 weighted 3D-sequence; volumetric isotropic turbo spin echo acquisition (VISTA) was taken parallel to the mid-sagittal plane.

*Results:* Comparing the two MR imagining protocols the acquisition time of the sagittal 3D sequence (6 min 42 s) was shorter than the total acquisition time of the 2D sequences (10 min 12 s) without jeopardizing the image quality or accuracy of the diagnostic information. MRI depicted the fistula in 94% (16 out of 17) of patients who were clinically proven fistulous, which is a privilege to detect associated anomalies on the same examination. The frequency of associated anomalies was 100% in high anorectal malformations (ARMs), 64% in intermediate and only 20% in low ARMs. From these associated anomalies vertebral anomalies were seen in 50% of patients. Concomitant cord anomalies were encountered in 60% of those with vertebral anomalies the most common of which was tethered cord observed in 35% of the patients.

*Conclusion:* MRI is a valuable diagnostic tool to diagnose type and level of ARM in addition to the privilege of associated anomalies detection on the same examination. The 3D sequence acquisition with multiplanar reconstruction has the advantage of time saving without compromise on image quality or the diagnostic accuracy compared to 2D images.



* Corresponding author. Mobile: +20 1223600583, +20 1123000552.
E-mail addresses: rania729@yahoo.com (R.F. Elsayed), Hebakamala@yahoo.com (H.A. Kamal), nevienelliethy@yahoo.com (N.E. El-Liethy).

Peer review under responsibility of The Egyptian Society of Radiology and Nuclear Medicine.

http://dx.doi.org/10.1016/j.ejrnm.2016.05.014

## 1. Introduction

Anorectal malformations (ARMs) comprise a wide spectrum of diseases that involve the distal anus, rectum as well as the urinary and genital tracts. The reported incidence is approximately 1/5000 live birth. The anomalies range from minor types that are easily treated with an excellent functional prognosis to those that are complex and difficult to manage, and have a poor functional prognosis (1).

ARMs are usually categorized according to the level of the rectal pouch relative to the levator ani muscles, and are thus described as high, intermediate, or low lesions. Most ARMs are of the communicating type, in which the enteric component issues into the urinary or genital tract or to the perineum. Less commonly the rectum ends blindly. A rare complex of anomalies, exclusively found in phenotypic girls, is the cloacal malformation, in which the urinary, genital, and intestinal tracts converge into a common cavity, i.e., the cloaca (2).

ARMs are frequently associated with other anomalies, particularly of the spinal cord, spine, and urogenital system, as reflected in the acronyms VACTERL (Vertebral anomalies, anal atresia, cardiac malformations, tracheo-esophageal fistula, renal anomalies, and limb anomalies) (2).

Magnetic resonance imaging (MRI) has proven to be of considerable value in evaluating patients with ARMs, especially because of its multiplanar imaging capability and superb tissue characterization. MRI allows accurate definition of the level and type of ARMs, type of fistula, and developmental state of the sphincter muscle complex. An additional advantage of MRI over other imaging modalities is its ability to determine associated anomalies, especially of the spinal cord, spine and the urogenital system (3).

Multiplanar reformatting (MPR) technique is one of the latest techniques in the post processing technologies. A 3D Turbo Spin Echo (TSE) sequence such as (FSE-XETA, T2-SPACE, and VISTA) can serve as a source data for post-processing reconstruction of images into any desired plane. Therefore a single 3D sequence with post processing reconstruction of images in the axial, coronal, and sagittal planes can potentially replace 2D sequences in those three planes, decreasing the number of sequences performed from three to one (4).

**Table 2** Pena classification (7).

| Male defects | Female defects |
|---|---|
| • Perineal fistula | • Perineal fistula |
| • Rectourethral bulbar fistula | • Vestibular fistula |
| • Rectourethral prostatic fistula | • Imperforate anus with no fistula |
| • Rectovesical (bladder neck) fistula | • Rectal atresia and stenosis |
| • Imperforate anus without fistula | • Persistent cloaca |
| • Rectal atresia and stenosis | < 3 cm common channel |
| | > 3 cm common channel |

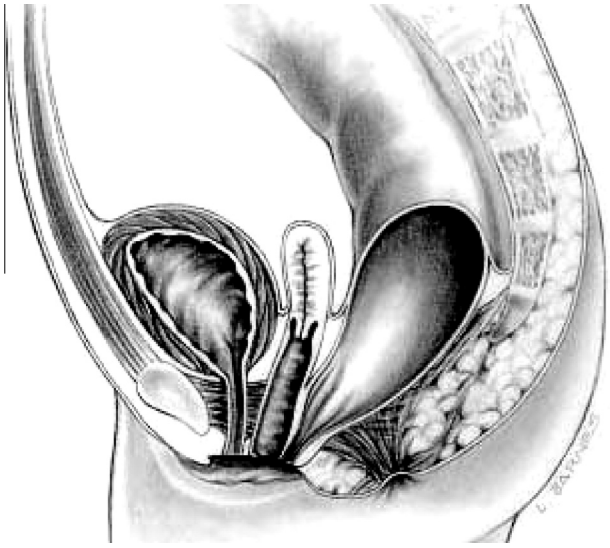

**Fig. 1** Rectovestibular fistula in females (8).

## 2. Materials and methods

### 2.1. Patients

The study group consisted of 20 patients with anorectal anomalies age range (2 months–3.5 years). All patients were referred to the Radiology department from the pediatric surgery unit between November 2013 and August 2014. These

**Table 1** Wingspread international classification (6).

| | Female | Male |
|---|---|---|
| High | | • Anorectal agenesis– Rectovesical fistula<br>– Rectoprostatic fistula<br>– No fistula<br>• Rectal atresia |
| Intermediate | • Rectovaginal fistula<br>• Rectovestibular fistula<br>• Anal agenesis without Fistula | • Rectobulbar fistula<br>• Anal agenesis without fistula |
| Low | • Anovestibular fistula<br>• Anocutaneous fistula<br>• Anal stenosis | • Anocutaneous fistula<br>• Anal stenosis |
| Cloaca | Cloaca | – |
| Rare | Rare malformations | Rare malformations |

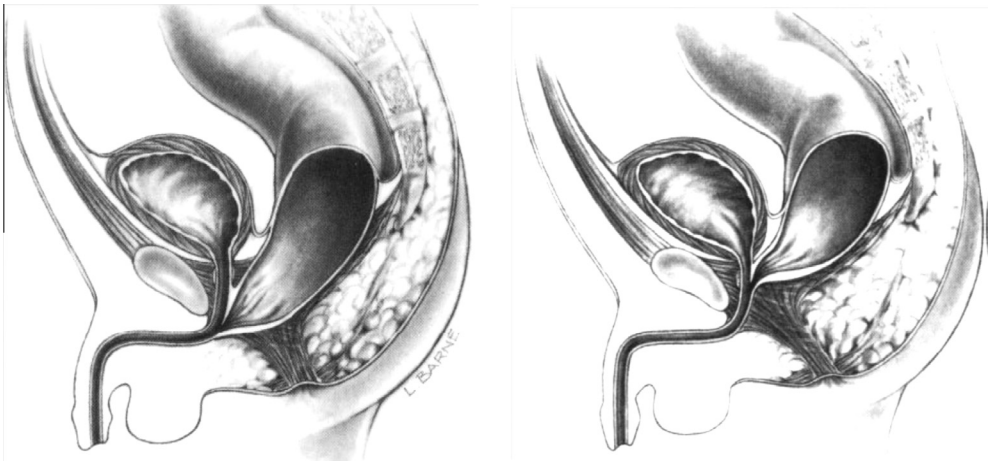

**Fig. 2** Rectourethral fistula (9).

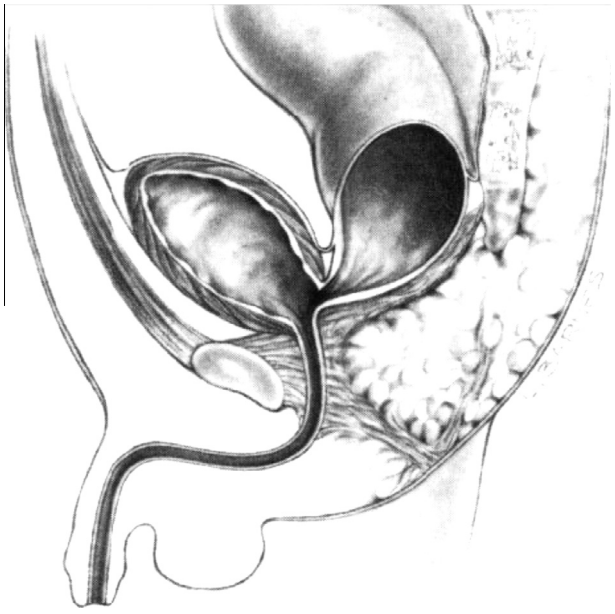

**Fig. 3** Rectovesicle fistula (9).

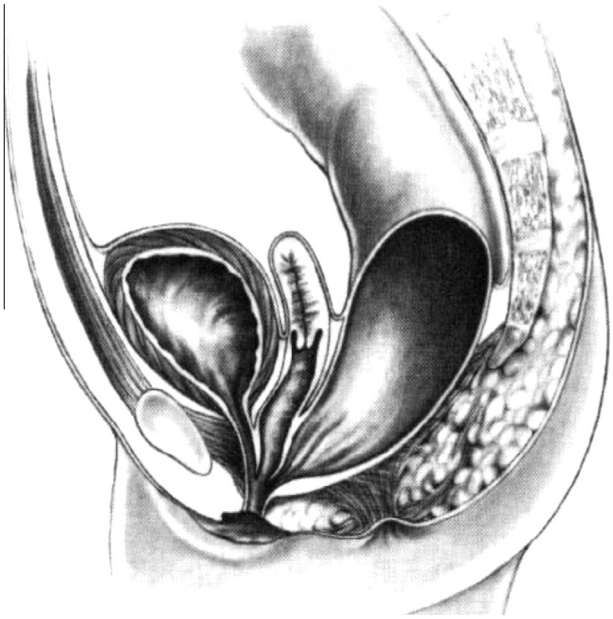

**Fig. 4** Persistent cloaca (9).

patients were scheduled for anorectoplasty and MRI was performed pre-operatively.

The study was approved by our institution's review board, and informed consent was obtained from all participants.

### *2.2. Magnetic resonance imaging*

MR imaging was performed using Intera 1.5 T MRI scanner (Philips medical systems, Best, the Netherlands). Head coil (C1) was used for infants (< 1 year old) and body phased-array coil (SENSE-XL-TORSO) for older children. No oral or intravenous contrast agent was administrated.

#### *2.2.1. 2D MR imaging sequences*

Images of the pelvis to assess the level and type of ARM as well as the bulk of the sphincter muscle complex were acquired in the three orthogonal planes by using T2-weighted Turbo Spin-Echo (T2W TSE) sequences (repetition time msec/echo time msec, **5000/132**; field of view, **130–150**; section thickness, **1.5 mm**; gap, **1 mm**; number of signals acquired, **2**; flip angle, **90°**; matrix, **512 × 512**; acquisition time, **3.12 min** for each sequence).

In the coronal and axial section orientation was parallel and perpendicular to the plane of the anal canal (5).

In addition, 2D sagittal and coronal T2W TSE (repetition time msec/echo time msec, **5000/132**; field of view, **170–220**;

**Table 3** Different pathological types of anorectal anomalies by conventional imaging.

| No. of patients | Pathology |
|---|---|
| 3 (15%) | Cloaca |
| 2 (10%) | Rectourethral fistula |
| 4 (20%) | Anteriorly displaced anus (ADA) |
| 11(55%) | Vestibular fistula |

**Table 4** MRI findings in 20 patients with ARM.

| Case no. | Age/gender | Level of ARM | Type of ARM | EAS bulk | Associated congenital anomalies |
|---|---|---|---|---|---|
| 1 | 8 mo M | High | Rectoprostatic fistula | Fair | – Isolated coccygeal agenesis<br>– Tethered cord with filum lipoma |
| 2 | 7 mo M | Intermediate | Rectobulbar fistula | Good | Cardiac (diagnosed by Echocardiography) |
| 3 | 8 mo F | Intermediate | Rectovaginal fistula | Fair | – Hydronephrosis and hydroureter<br>– Isolated partial coccygeal agenesis |
| 4 | 9 mo F | Intermediate | Rectovestibular fistula | Good | Isolated partial coccygeal agenesis |
| 5 | 7 mo F | Intermediate | Rectovestibular fistula | Good | – Left renal agenesis<br>– Tethered cord<br>– Isolated partial coccygeal agenesis |
| 6 | 9 mo F | Intermediate | Rectovestibular fistula | Good | Isolated partial coccygeal agenesis |
| 7 | 1 year F | Intermediate | Rectovestibular fistula | Fair | _ |
| 8 | 7 mo F | Intermediate | Rectovestibular fistula | Good | _ |
| 9 | 8 mo F | Intermediate | Rectovestibular fistula | Good | _ |
| 10 | 11 mo F | Intermediate | Rectovestibular fistula | Good | _ |
| 11 | 9 mo F | Intermediate | Rectovestibular fistula | Fair | Isolated partial coccygeal agenesis |
| 12 | 5 mo F | Intermediate | Rectovestibular fistula | Fair | – Tethered cord<br>– Isolated partial coccygeal agenesis |
| 13 | 5 mo F | Low | Anovestibular fistula | Fair | – Tethered cord<br>– Partial sacral agenesis |
| 14 | 8 mo | Low | Anovestibular fistula | Good | _ |
| 15 | 2 mo F | Low | ADA | Good | _ |
| 16 | 5 mo F | Low | ADA | Good | _ |
| 17 | 7.5 mo F | Low | ADA | Good | _ |
| 18 | 2.3 year F | Cloaca | Type III | Fair | – Hemivertebra L4 with lumbar scoliosis<br>– Hemisacralized L5<br>– Partial sacra agenesis<br>– Tethered cord with filum lipoma<br>– Duplicated uterus, cervix and vagina |
| 19 | 3.5 year F | Cloaca | Type II | Poor | – Fused L4-L5 vertebral bodies (block vertebra)<br>– Partial sacral agenesis<br>– Hydronephrosis and hydroureter |
| 20 | 11 mo F | Cloaca | Type I | Good | Tethered cord |

section thickness, **5 mm**; gap, **2 mm**; number of signals acquired, **2**; flip angle, **90°**; matrix, **512 × 512**) was acquired for detection and diagnosis of associated congenital anomalies. In these sequences the large field of view was used to cover the lower border of the liver.

#### 2.2.2. 3D MR imaging sequences

3D MR images were acquired in the sagittal plane using T2 weighted; volumetric isotropic turbo spin echo acquisition (**VISTA**) taken parallel to the mid sagittal plane (TE, **275 ms**; TR, **1500 ms**; field of view, **170–220**; section thickness, **1 mm**; gap, **0 mm**; flip angle, **90°**; matrix, **512 × 512**, acquisition time **6.42 min**).

### 2.3. Data analysis

The MR imaging data sets were assessed by a radiologist (R.F. E.S., with 15 years of experience interpreting pelvic floor MR images). The radiologist was aware of each patient's clinical history and diagnosis.

Multi-planar Reconstruction (MPR) of the sagittal VISTA MR images was reconstructed on a graphic workstation (PHILIPS workstation) to generate reformatted images in the axial, coronal, and sagittal planes with slice thickness, inter-slice gap and orientations identical to those of the 2D TSE MR images. Each reformatted image was compared side by side with the corresponding 2D TSE image. All measurements were obtained with software (Dicom Works, version 1.3.5; http://dicom.online.fr/).

Analysis of the MR images was based on scrutiny of the following criteria:

1. Location of bowel termination and its type based on **Wingspread** classification 1984 (Table 1) in relation to the following:
   - PCL (**pubo-coccygeal line**; *extending from the upper border of the os pubis to the os coccyx* corresponds with the attachment of levator ani muscle to the pelvic wall, separating high-type malformations lying above the levator muscle and intermediate and low forms of anorectal agenesis lying below this anatomic line) (6).
   - I-plane (**ischeal plane**; *passing through the lowest point of the ischial tuberosity*, represents the deepest point of the funnel of the levator ani muscles, separating intermediate type malformations from low type above and below this line) (6).
2. The presence of fistula and its type based on Pena classification (Table 2) (7).

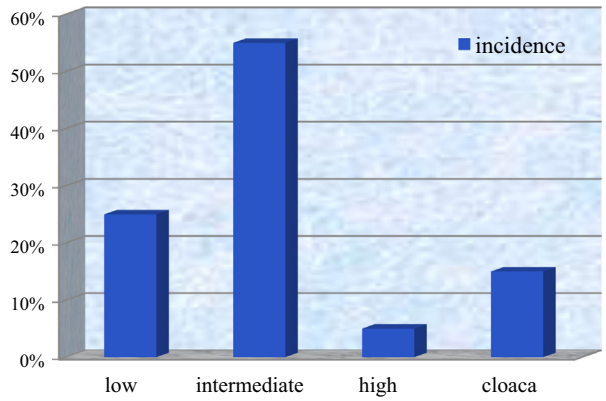


**Fig. 5** Chart showing the incidence rate of ARM according to their level.

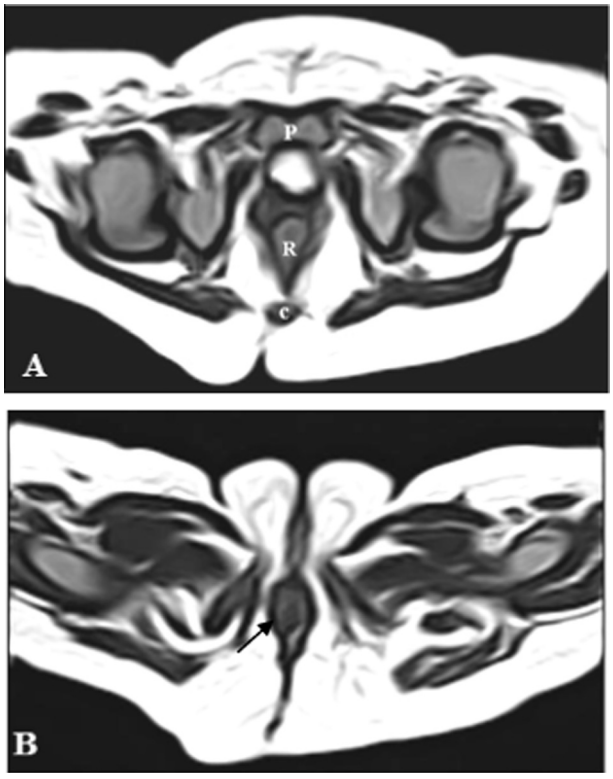


**Fig. 6** Axial TSE T2 WI (A) at the PC-plane, the rectal pouch (R) is seen. (B) At the I-plane, EAS is normally developed (arrow). Rectum is not seen, indicating intermediate ARM. P = pubic body, c = coccyx.

The most common anomaly in females is rectovestibular fistula (Fig. 1). In this defect, the bowel opens immediately behind the hymen in the vestibule of the genital system. Immediately above the fistula, the rectum and vagina are separated by a thin, common wall (8).

The most frequent variant seen in males is rectourethral fistula (Fig. 2). The fistula is located at or near the bulbar region of the urethra or near the prostatic urethra. Immediately superior, the rectum and urethra share a common wall (9).

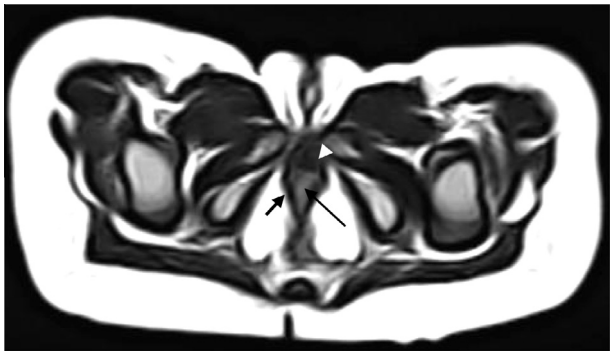

**Fig. 7** Axial TSE T2 WI showing the rectum (arrow) and the persistent urogenital sinus (arrowhead). Puborectalis muscle (small arrow) is seen as well.

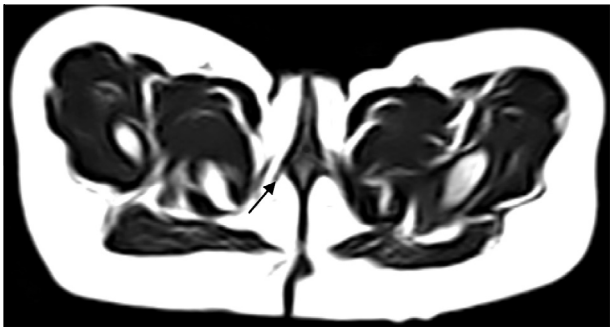

**Fig. 8** Axial TSE T2 WI showing the anus anterior to the superficial transverse perineal muscle (arrow). The orifice of the persistent urogenital sinus is seen ventral to the anus.

Rectovesical fistula: in this higher level defect, the rectum opens at the bladder neck (Fig. 3) (9).

Persistent cloaca: this malformation involves fusion of the rectum, vagina, and urethra together to form a common channel (Fig. 4) (9).

Anterior displaced anus (ADA) is a common malformation which is a forme fruste [mild, incomplete or atypical form] of imperforate anus (10). It is a normal appearing anal orifice, located in an abnormally anterior position, with an anal canal of normal caliber, which is surrounded 360° by the EAS (11). In girls, the posterior fourchette of the vagina (or scrotal–perineal junction in boys) could be used as a reference point (12).

3. The degree of development of the sphincter muscle complex in the coronal and axial planes.
   - The muscle bulk was graded as good if its thickness was within the average.
   - Fair if the muscle was clearly identified but thin.
   - Poor if the muscle complex was not identified.

4. Other associated anomalies involving the vertebrae, spinal cord and/or the genitourinary system anomalies.

Many of these associated anomalies are serious, and the long-term prognosis of children with anorectal malformations is often more dependent on the extent of these associated anomalies than on the anorectal malformation itself.

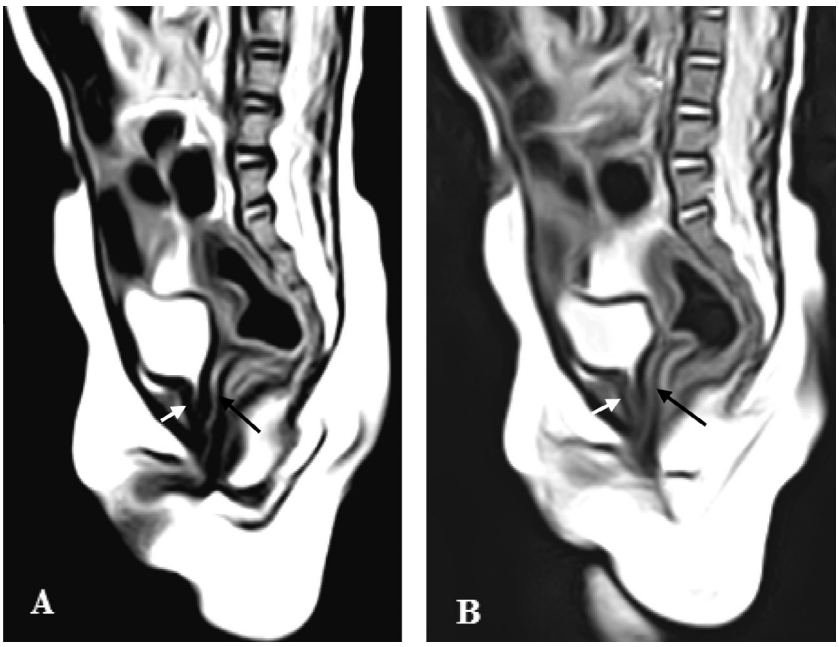


**Fig. 9** (A) Sagittal TSE T2 WI shows the rectovaginal fistula (long arrow). Urethra is seen as a separate tract (short arrow). (B) The corresponding sagittally reconstructed image from the 3D sequence image.

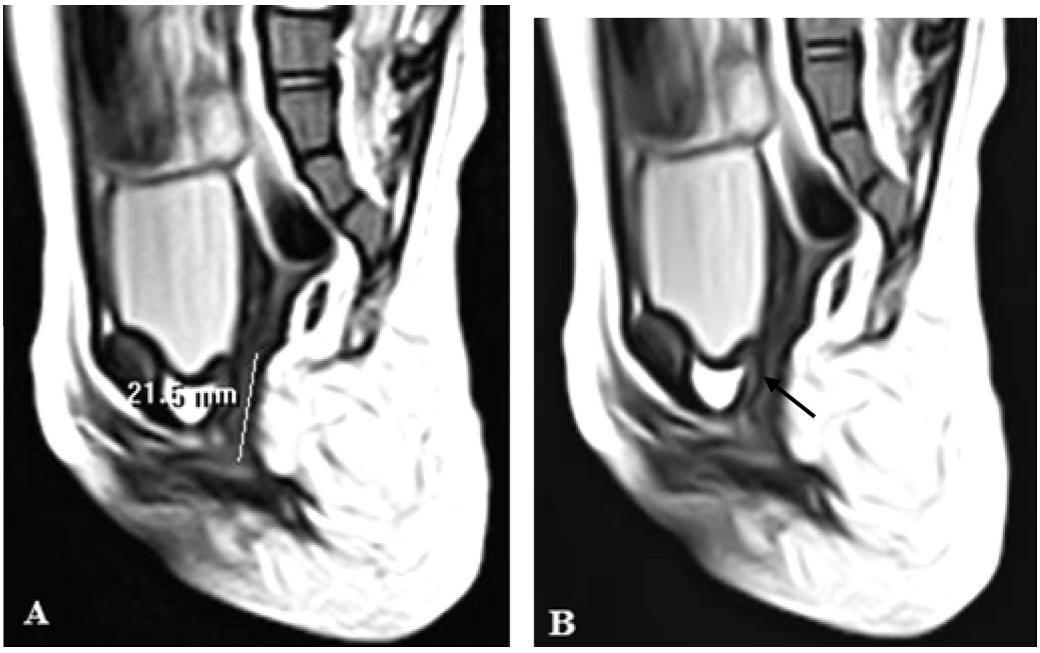


**Fig. 10** (A) 2D-TSE sagittal T2 WI and (B) the 3D-VISTAT2 WI in sagittal plane, both showing the entrance of the rectum into the urogenital sinus (arrow) and the short common channel (2.15 cm) indicating type II cloaca.

They are twice as common with high, as opposed to low, anorectal malformations. Spinal cord, spine, and urogenital system are the most commonly involved whereas esophageal atresia and congenital heart disease are also frequently encountered (2).

## 3. Results

On clinical examination the most common ARM was vestibular fistula 11 (55 %). The 20 patients with anorectal anomalies included in this study were diagnosed clinically and by conventional imaging into the following pathological types (Table 3).

*The level of ARM* and bowel termination in relation to the pelvic diaphragm was correctly diagnosed in all patients with MRI when compared to operative data (Table 4 and Fig. 5).

In one patient, conventional imaging was inaccurate in determining the ARMS level, and distal loopogram of this patient showed the rectal pouch above the PC plane while MRI defined its location below the PC plane making the diagnosis of intermediate ARMS (Fig. 6).

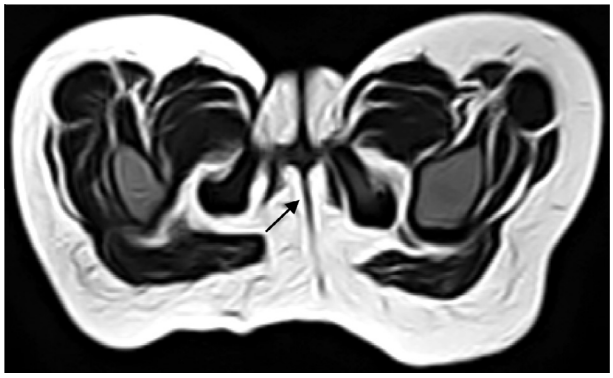

**Fig. 11** Axial TSE T2 WI at the PC-plane shows the poorly developed EAS (arrow).

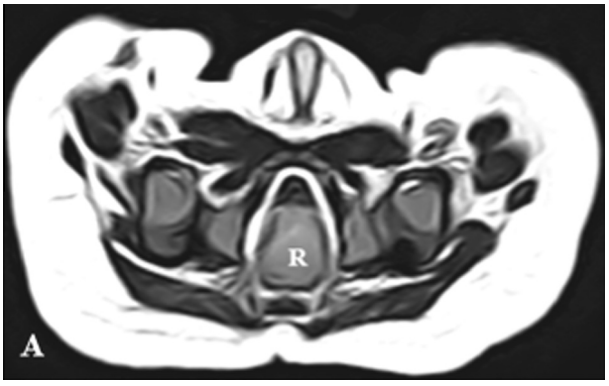


**Fig. 12** Axial TSE T2 WI (A) at PC-plane, the rectal pouch (R) is seen. No fistulous tract between prostatic urethra and rectum.

***Type of ARMS***: preoperative MRI helped also in accurately determining the type of ARMS. Patient no. 2 was diagnosed clinically as ADA while her MRI study revealed the presence of a persistent urogenital sinus along with the ADA, making the diagnosis of type I cloaca (Figs. 7 and 8).

Patient no. 4 was for surgery as case of cloaca; however, visualization of a separate urethral tract by MRI made the diagnosis to be changed into rectovaginal fistula. The MR diagnosis was confirmed operatively (Fig. 9).

In patients with cloaca MRI accurately located the position of union of the rectum with urogenital sinus in relation to PC line which accurately determined the type of cloaca either long channel or short channel (Figs. 10 and 11).

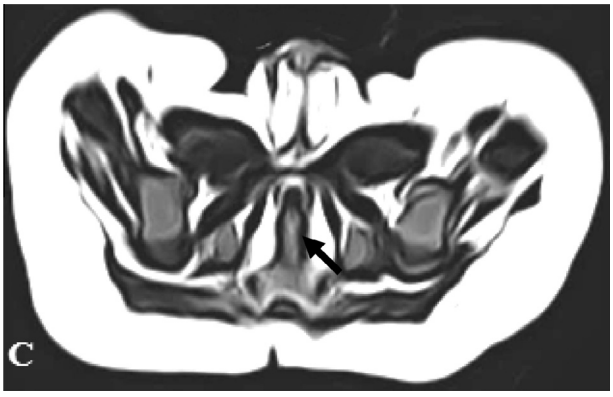


**Fig. 14** Axial image reconstructed from the 3D data set image showing the rectobulbar fistula with similar quality as in the 2D TSE acquired images.

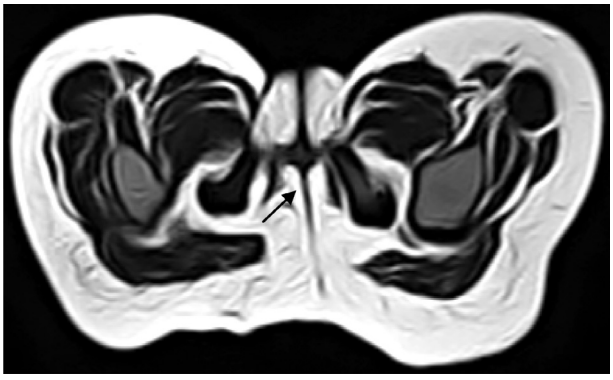

**Fig. 15** Axial TSE T2 WI at the PC-plane shows the poorly developed EAS (arrow).

*Fistula*: Patient no. 6 was said to have recto-prostatic urethra fistula, based on his preoperative distal loopogram. However his MRI revealed rectobulbar fistulous tract, which was confirmed operatively (Figs. 12–14).

*The anal sphincter muscle complex (SMC)* was directly visualized with MRI, and assessment of its bulk, which reflects its developmental state, was evaluated in axial and coronal planes (Figs. 15 and 16).

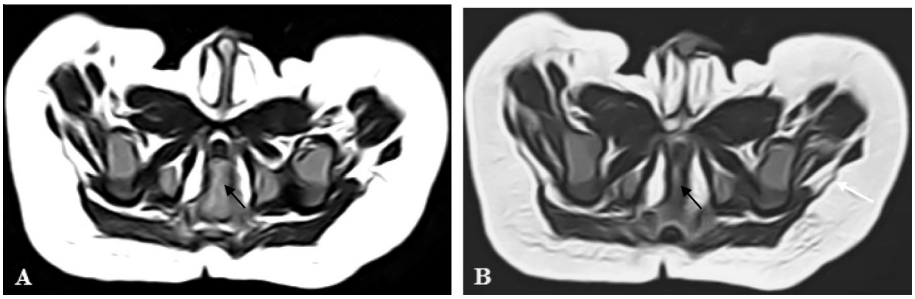


**Fig. 13** (A) and (B) Axial TSE T2 WI showing the recto-bulbar uretheral fistula as linear tract lined by the hyperintense rectal mucosa (arrow).

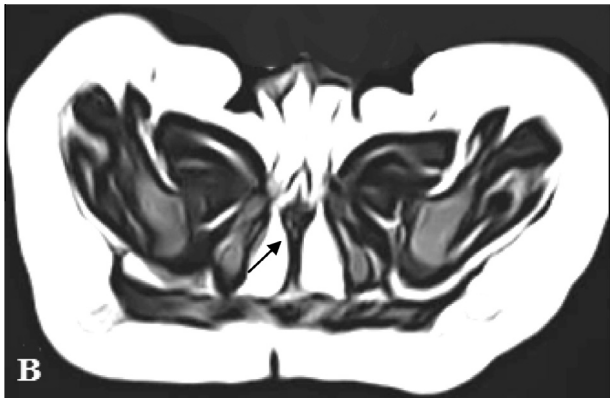


**Fig. 16** Axial TSE T2 WI (B) at I-plane, shows the EAS is of average bulk.

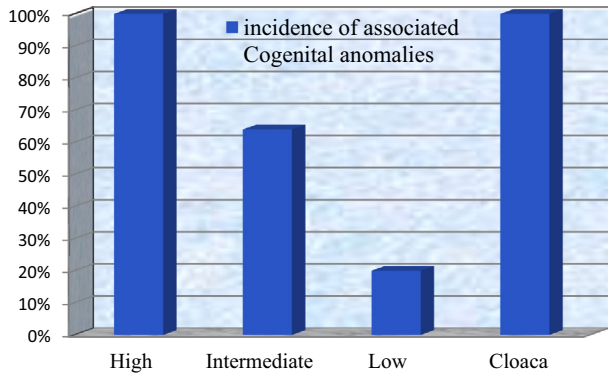


**Fig. 17** Chart showing incidence of associated anomalies among different groups of ARMS.

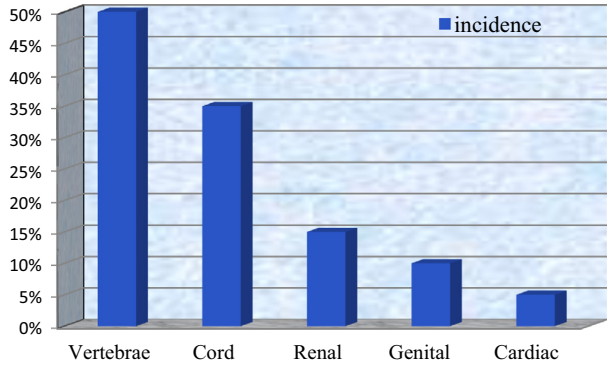


**Fig. 18** Chart showing incidence of associated anomalies according to the organ/system involved.

Evaluation of the *associated congenital anomalies* revealed 12 out of the 20 patients (60%) having other anomalies involving the spine, spinal cord, urogenital system and CVS. Details of these associated anomalies are summarized in Table 5, Figs. 17 and 18.

Out of the 20 patients 2 (10%) had genital anomalies and both were patients with persistent cloaca. Patient with short channel cloaca had a longitudinal septum in the proximal vagina. Patient with long cloaca had duplication of the vagina, cervix and uterus (Figs. 19 and 20).

### *3.1. Multi-planar Reconstruction (MPR) of the sagittal VISTA versus 2D MR images*

In comparison with the reconstructed images from the 3D data set images and the acquired 2D images, there were no differences as regards image quality and accuracy of the diagnostic information obtained (Fig. 10). Both types of images agreed as regards the diagnosis of the ARMs levels and types, detection of fistulae, assessment of sphincter muscle bulk and detection of the associated congenital anomalies.

The acquisition time for the sagittal 3D TSE sequence was 6 min 42 s (±35 s). The overall acquisition time of the 2D

**Table 5** Summary of associated congenital anomalies.

| System involved | Anomaly | No. of cases | ARM level |
|---|---|---|---|
| Vertebral column | Isolated partial coccygeal agenesis | 7 | 1 high<br>6 intermediate |
| | Partial sacral agenesis with missing coccygeal segment | 3 | 1 high<br>1 intermediate<br>1 low |
| | L4 hemi-vertebra<br>Hemi-sacralized L5 | 1 | Cloaca |
| | Block vertebra (fused L4 and L5) | 1 | Cloaca |
| Spinal cord | Tethered cord with filum terminal lipoma in 2 cases | 6 | 2 high<br>3 intermediate<br>1 low |
| | Distal cord agenesis | 1 | Low |
| | Distal cord agenesis | 1 | Low |
| Urologic | Unilateral renal agenesis | 1 | Intermediate |
| | Hydro-nephrosis and ureter | 2 | Intermediate |
| Genital | Duplicated uterus, cervix and vagina | 1 | Cloaca |
| | Vaginal septum | 1 | Cloaca |
| CVS | VSD | 1 | Intermediate |

sequences was 10 min, 12 s (±49 s). Our results show that the acquisition time of the 3D VISTA sequence is notably shorter than that of the 2D sequences collectively.

## 4. Discussion

Accurate evaluation of patients with anorectal anomalies involves correct assessment of the level and type of malformation, the existence of fistula, the developmental state of the sphincter muscle complex, and the presence of associated anomalies. This information is essential in planning initial management, as well as predicting morbidity, quality of life and prognosis of survival (2).

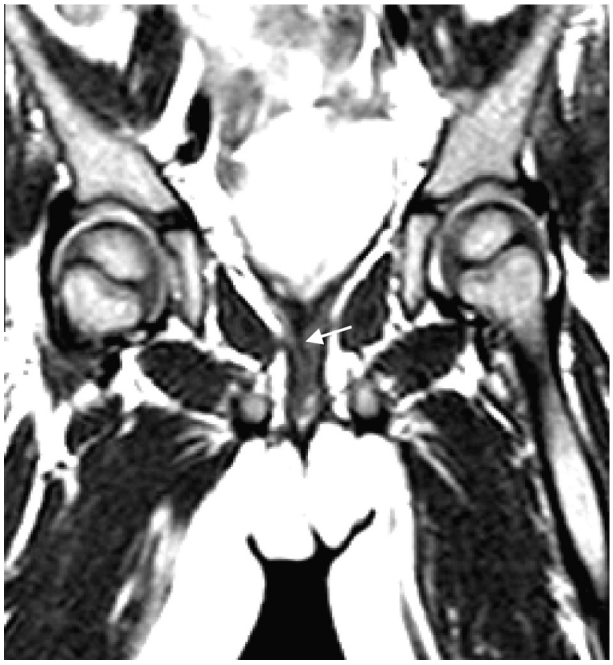

**Fig. 19** Coronal TSE T2 WI shows a longitudinal septum in the proximal vagina (arrow).

In this study we performed preoperative MRI assessment for 20 patients ranging in age from 2 months to 3.5 years. We acquired triplanar 2D MRI series and reconstructed corresponding series from 3D data set images, and compared their results against the patient's operative data. To our knowledge few studies in the literature had investigated the role of preoperative MRI in evaluating patients with anorectal malformation (13–15,2).

We found that MRI was more accurate than conventional imaging in determination of the type and level of aneorectal anomaly in the preoperative patients. MRI also accurately depicted the fistula in 94% (16 out of 17) patients who had clinically proven fistulae. Similar results were found in the study conducted by (14,2).

The inaccuracy in the clinical and conventional imaging diagnoses may be attributed to difficulty of perineal inspection in infant patients, and to some technical faults that might occur while doing the distal loopogram and cloacogram. The recommended high pressure technique used in the distal loopogram to enhance visualization of recto-urogenital fistula may cause distension and descent of the rectal pouch, leading to a false impression of a lower anomaly. In contrast, doing the examination with an inadequately prepared rectum gives a false impression of higher level anomaly (2).

Regarding the anal musculature, MRI allowed direct visualization of sphincter muscle complex in multiple planes facilitating accurate evaluation of its bulk size and location. This agrees with (13,15,2).

It is well known that additional congenital anomalies are often present in patients with anorectal anomalies, and it is

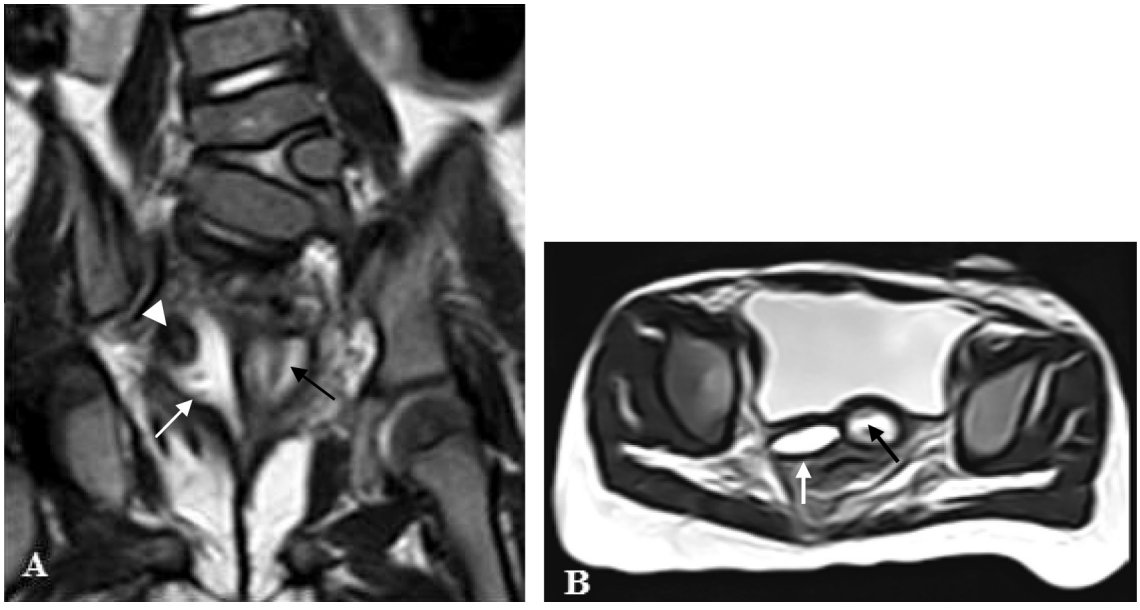


**Fig. 20** (A) Coronal TSE T2 WI and (B) axial TSE T2 WI showing duplication of the vagina, cervix and uterine cavity. A well developed uterus on the left (black arrow) and rudimentary one on the right (arrow head), hydrocolpos (white arrow) may indicate the presence of a transverse vaginal septum.

these coexisting anomalies that account for the high morbidity and mortality associated with this condition (16). We found that MRI was able, on the same examination to detect associated anomalies especially of the spinal cord, and urogenital system. This coincides with Nievelstein et al. (2).

High type ARMS are more frequently associated with other congenital anomalies than low type lesions (16,17). This was the observation in our study, where the frequency of associated anomalies was 100% in high ARMS, 64% in intermediate and 20% in low ARMS.

Vertebral anomalies were seen in 50% of the patients included in our study. The presence of concomitant cord anomalies was encountered in 60% of those with spinal anomalies. Same figures of incidence rate were reported by Nievelstein et al. (2) in his study.

The reported prevalence of spinal cord abnormalities in patients with ARMS varies between 10%, 50% and more (18,19). The most common associated spinal dysraphic anomaly is the tethered cord. It was observed in approximately 35% of children with ARMS in the study by (20–22). We got comparable results in our study, with prevalence of spinal cord anomalies of 35% and the tethered cord being the most commonly encountered anomaly with a prevalence rate of 30%.

Genitourinary anomalies were found in 25% of the patients, which is close to the results of previous reviews that report incidences from 30% to 40% (23,24).

In this study we investigated the difference between the 2D images acquired in different planes and the post-processing reconstructions generated from a single 3D VISTA sequence data set. Our results showed that the acquisition time of the sagittal 3D sequence (6 min 42 s) is notably shorter than the total acquisition time of the required 2D sequences. Otherwise, there was no significant difference between the 3D and 2D images in regard to image quality and accuracy of the diagnostic information obtained. Unfortunately, no similar studies on the pediatric age group, neither on patients with ARMS were found. However, Proscia et al. (4) have done a similar study on the pelvic region in women. He has investigated the role of 2D versus 3D MR images in diagnosis of different female pelvis pathologies and his result was comparable to ours.

Therefore the post-processing generation of multiplanar reconstructions from 3D data set can potentially replace 2D sequences in different planes, decreasing the examination time without compromise on image quality or accuracy. This is considered to be crucial importance in the pediatric age group, since they need to be sedated during the examination.

Limitations of our study included the use of sedation and apparent high cost of MRI relative to conventional investigations.

In conclusion, MRI is a valuable diagnostic imaging modality in identifying the multiple aspects of ARMS. It has more accurate results to conventional investigations in preoperative patients.

The 3D sequence acquisition with multiplanar reconstruction generation is a promising tool for imaging. As compared to the 2D images acquired in various planes, it has the privilege of time saving without compromise on image quality or the diagnostic information obtained, and the versatility of reconstructing images in any orientation.

## Conflict of interest

We have no conflict of interest to declare.

## References


(1) Senel E, Akbiyik F, Atayurt H, et al. Urological problems or fecal continence during long term follow-up of patients with anorectal malformations. Pediatr Surg Int 2010;26:683–9.
(2) Nievelstein RAJ, Vos A, Valk J, et al. Magnetic resonance imaging in children with anorectal malformations: embryologic implications. J Pediatr Surg 2002;37:1138–45.
(3) Kluth D. Embryology of anorectal malformations. Semin Pediatr Surg 2010;19:201–8.
(4) Proscia N, Jaffe TA, Neville AM, et al. MRI of the pelvis in women: 3D versus 2D T2-Weighted Technique. AJR 2010;195:254–9.
(5) El Sayed RF, Mashed SE, Farag A, et al. Pelvic floor dysfunction: assessment with combined analysis of static and dynamic MR imaging findings. Radiology 2008;248:518–30.
(6) Holschneider A, Hutson J, Pena A, et al. Preliminary report on the international conference for the development of standards for the treatment of anorectal malformations. J Pediatr Surg 2005;40:1521–6.
(7) Rintala RJ. Anorectal malformations management and outcome. Sem Neonatol 1996;1:219–30.
(8) Levitt MA, Peña A. Anorectal malformations. Orphaned J Rare Dis 2007;2:33–46.
(9) Pena A. Atlas of surgical management of anorectal malformations. New York: Springer-Verlag; 1992.
(10) Pena A. Comment on anterior ectopic anus. Pediatr Surg Int 2004;20:902.
(11) Thambidorai CR, Raghu R, Zulfiqar A, et al. Magnetic resonance imaging in anterior ectopic anus. Pediatr Surg Int 2008;24:161–5.
(12) Herek O, Polat A. Incidence of anterior displacement of the anus and its relationship to constipation in children. Surg Today 2004;34:190–2.
(13) Sato Y, Pringle KC, Bergman R, et al. Congenital anorectal anomalies: MR imaging. Radiology 1988;168:157–62.
(14) McHugh K. The role of radiology in children with anorectal anomalies; with particular emphasis on MRI. Eur J Radiol 1998;26:194–9.
(15) Aslam A, Grier DJ, Duncan AW, et al. The role of magnetic resonance imaging in the preoperative assessment of anorectal anomalies. Perdiatr Surge Int 1998;14:71–3.
(16) Cho S, Moore SP. Fangman one hundred three consecutive patients associated anomalies. Arch Pediatr Adolesc 2001;155:587–91, with anorectal malformations and their.
(17) Endo M, Hayashi A, Ishihara M, et al. Patients with anorectal malformations over the past two decades in Japan. J Pediatr Surg 1999;34:435–41.
(18) KrauB J, Schropp C. Tethered spinal cord in patients with anorectal malformations. In: Hutson JM, Holschneider AM, editors. Anorectal malformations in children, embryology, diagnosis, surgical treatment and follow up. Berlin Heidelberg: Springer-Verlag; 2006.
(19) Tuuha SE, Aziz D, Drake J, et al. Is surgery r asymptomatic tethered cord in anorectal malformation patients? J Pediatr Surg 2004;39:773–7.
(20) Long FR, Hunter JV, Mahboubi S, et al. Tethered cord and associated vertebral anomalies in children and infants with

imperforate anus: evaluation with MR imaging and plain radiography. Radiology 1996;200:377–82.
(21) Sato S, Shirane R, Yoshimoto T, et al. Evaluation of tethered cord syndrome associated with anorectal malformations. Neurosurgery 1993;32:1025–8.
(22) Warf BC, Scott RM, Barnes PD, et al. Tethered spinal cord in patients with anorectal and urogenital malformations. Pediatr Neurosurg 1993;19:25–30.
(23) Wagner BJ, Woodward PJ. Magnetic resonance evaluation of congenital uterine anomalies. Semin Ultrasound CT MR 1994;15:4–17.
(24) Boechat MI. Magnetic resonance imaging of the pediatric pelvis. Radiol Clin North Am 1992;30:807–16.